Mechanism of ethylene hydroformylation on platinum complexes with hydrophosphoryl ligands: a DFT study

Yu. A. Ustynyuk,[a] Yu. V. Babin,[b] V. G. Savchenko,[b] E. M. Myshakin,[b] and A. V. Gavrikov[a]*

[a]*Department of Chemistry, M. V. Lomonosov Moscow State University, Bldg. 3, 1 Leninskie Gory, 119992 Moscow, Russian Federation. Fax: +7 (495) 939 2677. E-mail: ustynyuk@nmr.chem.msu.su*
[b]*Pacific State University of Economics, 19 Okeanskiy prosp., 690091 Vladivostok, Russian Federation. Fax: +7 (423 2) 40 6634. E-mail: buv@list.ru*

The mechanism of ethylene hydroformylation on model organoplatinum hydrides $[(R_2PO)_2H]Pt(PR_3)(H)]$ (R = H, Me, CF_3) was studied within the framework of the density functional theory with the PBE gradient-corrected functional and the TZ2p basis set. The presence of a free coordination site in these square-planar 16-electron platinum complexes provides the possibility of alkene coordination in the first step without energetically unfavorable dissociation of one of the metal—ligand bonds. High strength of the $-PR_2O-H\cdots O-PR_2$ hydrogen bond results in the formation of a bidentate ligand in the coordination sphere of the metal atom. This ligand makes the geometry of the catalytic center rigid, thus enhancing the regioselectivity of the process. The proton can reversibly migrate with ease within the $-PR_2O-H\cdots O-PR_2$ hydrogen bond, thus providing fine adjustment of the electron density in the catalytic center in each reaction step and acting as a molecular switch. The rate-limiting step in the hydroformylation is the CO insertion into the Pt—Et σ-bond. Electron-donating Me groups at the phosphorous atoms hamper, while electron-withdrawing CF_3 groups facilitate, the process.

Key words: homogeneous metal complex catalysis, hydroformylation of alkenes, hydrogenation, hydrophosphoryl ligands, quantum chemical calculations, *ab initio* quantum chemical calculations, density functional theory, MP2 method, catalytic cycle.

Hydrophosphoryl compounds (HPC) occupy a special position in chemistry of organophosphorus compounds. In solutions, they can undergo a tautomeric transition between two forms, a secondary phosphine oxide **1** and phosphinous acid **2**, which in turn can exist as a mixture of two rotamers, *trans*-**2** (**2a**) and *cis*-**2** (**2b**), as shown in Eq. (1). Owing to easy interconversion **1** ⇄ **2**, HPC exhibit a unique combination of the properties and reactivity of two main classes of organophosphorus compounds (derivatives of penta- and trivalent phosphorus), thus being attractive reactants for organic and organoelement synthesis.[1—3]

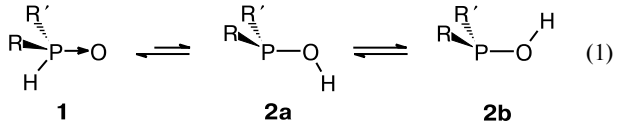

1 **2a** **2b** (1)

R, R′ = alkyl, aryl, alkoxy, aroxy.

In reactions of phosphine oxides with transition metal ions, the tautomeric equilibrium (see Eq. (1)) is shifted toward phosphinous acids, which, similarly to tertiary phosphines, form strong complexes with these ions.[4] This gave a new strong impetus to the development of the chemistry of HPC. Some aspects of coordination chemistry of HPC were reviewed.[5,6]

Higher stability of HPC against oxidation is their undoubtful advantage as ligands over tertiary phosphines traditionally used in catalysis; as a consequence, complexes of HPC are stable in air.[7] Phosphinous acids in the coordination sphere of metal atoms can be deprotonated with ease even under the action of weak bases (Eq. (2)).

$$[L_nM(PR_2OH)_2] + B \longrightarrow [L_nM(PR_2O)(PR_2OH)]^- + BH^+ \quad (2)$$

3

Therefore, complexes **3** act as active and stable catalysts of cross-coupling in, *e.g.*, the Kumada—Tamao—Corriu[7] and Suzuki—Miyaura[8] reactions; this allows one to use low-reactive substrates in these reactions. Two singly deprotonated phosphinous acid molecules in the inner co-

Published in Russian in *Izvestiya Akademii Nauk. Seriya Khimicheskaya,* No. 4, pp. 672—680, April, 2010.
1066-5285/10/5904-0686

ordination sphere of a metal atom can form complexes **4** where they act as chelating bidentate monoanion ligands. Such complexes are active and selective catalysts in the hydroformylation of alkenes[9] and hydrophosphinylation of alkynes.[10] Chiral complexes of HPC based on secondary phosphites containing chiral phosphorus atoms were also synthesized and studied.[11–13]

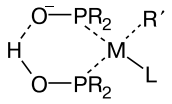

4

M = Pd, Pt; R = Me, Ph; R′ = H; L = PPh_3

Hydroformylation of alkenes under homogeneous conditions (Eq. (3)) is a key synthetic procedure in large-scale production of aldehydes. Traditionally used catalysts of this reaction include cobalt, rhodium, and palladium complexes. Cobalt carbonyls allow one to synthesize the target linear aldehydes in yield of up to 95%; however, in this case a significant drawback is the need for the use of high temperatures and pressures.

$$RCH{=}CH_2 + CO + H_2 \longrightarrow RCH_2CH_2CHO \qquad (3)$$

Hydroformylation in the presence of rhodium complexes proceeds under much milder conditions. but the process is accompanied by the formation of large amounts of branched aldehydes. The regioselectivity of the process can be improved using bidentate ligands,[14] which, however, are often more expensive than the metal.

The regioselectivity of hydroformylation of hept-1-ene using a type-**4** platinum(II) complex $[(Ph_2PO)_2H]Pt(PPh_3)(H)$ (**5**) as a catalyst under mild conditions is more than 90%.[9,15] Complex **5** is formed in solution *in situ* by simply mixing $Pt(cod)_2$ (cod = cycloocta-1,5-diene), PPh_3, and $Ph_2P(O)H$. In addition, the oxidative addition of diphenylphosphine oxide to $Pt(PEt_3)_3$ (see Ref. 10) also smoothly affords the complex $[(Ph_2PO)_2H]Pt(PEt_3)(H)$ (**6**) whose structure was established by X-ray diffraction analysis. Complex **6** is an active catalyst of hydrophosphinylation of alkynes.

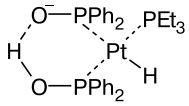

6

Earlier, the mechanism of hydroformylation of alkenes has theoretically been studied using various quantum chemical methods including MP2 (see Refs 16, 17) and DFT.[18–20] Both particular steps[16,17,19] and complete catalytic cycles[18,20] were studied. According to calculations, the limiting step of the overall process is the elimination of carbon monoxide (first step) for the $HCo(CO)_4$-catalyzed reaction[18] and the CO insertion into the metal—alkyl σ-bond for the reaction catalyzed by $HRh(CO)(PR_3)_3$.[20]

The course of the hydroformylation of hept-1-ene on complex **5** in a stepwise mode was studied in detail under controlled conditions.[9] As hept-1-ene was passed through a solution of compound **5** at 25 °C, NMR monitoring revealed the formation of a η^1-alkyl complex **7** (Eq. (4)). Subsequent passage of CO through the solution led to transformation of **7** to a η^1-acyl complex **8** (Eq. (5)) whose reaction with molecular hydrogen resulted in octanal as the final product (Eq. (6)).

$$\underset{\mathbf{5}}{L_3Pt{-}H} + C_5H_{11}CH{=}CH_2 \longrightarrow \underset{\mathbf{7}}{L_3Pt{-}CH_2CH_2C_5H_{11}} \qquad (4)$$

$$\underset{\mathbf{7}}{L_3Pt{-}CH_2CH_2C_5H_{11}} + CO \longrightarrow \underset{\mathbf{8}}{L_3Pt{-}COCH_2CH_2C_5H_{11}} \qquad (5)$$

$$\underset{\mathbf{8}}{L_3Pt{-}COCH_2CH_2C_5H_{11}} + H_2 \longrightarrow \underset{\mathbf{5}}{L_3Pt{-}H} + C_5H_{11}CH_2CH_2COH \qquad (6)$$

$L_3Pt{-}H$ = $[(Ph_2PO)_2H]Pt(PPh_3)(H)$ (**5**)

We carried out a detailed theoretical study of ethylene hydroformylation on the model complexes $[(R_2PO)_2H]Pt(PR_3)(H)$ with R = H (**9**), Me (**10**), and CF_3 (**11**) in order to reveal the main factors responsible for high efficiency of the type-**5** complexes in this reaction. This is of undoubtful interest for optimizing the molecular structures of this type of catalysts for their practical use. The preliminary results were reported elsewhere.[21]

Calculation Procedure

The molecular and transition-state geometries were fully optimized within the framework of the density functional theory. Calculations were carried out with the PBE gradient-corrected functional,[22] the TZ2P triple-zeta basis set[23,24] for the valence electrons, and the SBK-JC pseudopotentials[25,27] for the core electrons. Thermodynamic functions were calculated in the rigid rotator—harmonic oscillator approximation and the stationary point energies were obtained from calculations with inclusion of zero-point vibrational energy correction. In all cases, the correspondence between the transition states and initial compounds and reaction products was verified by constructing the intrinsic reaction coordinates (IRC). All calculations were performed in a parallel mode on supercomputer clusters at the Joint

SuperComputer Center (Moscow, Russia) using the PRIRODA program.[24] The potential energy surface (PES) of compound **9** in the vicinity of the global minimum was also studied using the B3LYP hybrid functional with the same basis set and by the MP2 (SDD/6-31G(d,p)) method.

Results and Discussion

Structures of type-5 hydrides. The calculated geometric parameters of complex hydrides **5**, **6**, and **9—11** as well as the experimental data[10] for compound **6** are listed in Table 1.

To check the correctness of the method used for calculations of the geometric parameters of this type of hydrides, we additionally calculated the structures of the complexes $[HPtZ(PPh_3)_2]$ (Z = CH_2CN, CF_3, Br) for which reliable X-ray data are available.[28—30] The results of these calculations and the corresponding experimental data are listed in Table 2.

By and large, the three computational methods used (DFT/PBE, DFT/B3LYP and MP2) provide a reasonable agreement with the X-ray data. They correctly reproduce the geometry of the coordination site, *viz.*, a distorted square in which the bidentate ligand $[(R_2PO)_2H]^-$ comprising a phosphinous acid molecule and its anion has a pronounced nonsymmetric structure with the hydrogen atom at the oxygen atom of phosphinous acid located in *trans*-position relative to the hydride. The coordination bond between this ligand and the metal atom is elongated. Calculations of the complexes $[HPt(Z)(PPh_3)_2]$ (Z = CH_2CN, CF_3, Br) reproduce the bond lengths and bond angles with a reasonable accuracy. For instance, the largest deviation (2.4°) was obtained for the P—Pt—P angle in the complex with Z = CF_3. The Pt—P distances differ by at most 0.05 Å (*cf.* a value of 0.12 Å for the Pt—C distances). As should be expected, the largest deviations were obtained for the Pt—H distances for which the errors in determination by X-ray analysis are the largest.

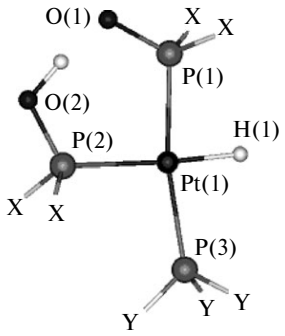

5—11

The PES of compound **9** exhibits no local minimum corresponding to proton location at the oxygen atom O(1). All the three computational methods showed that migration of this proton from the O(2) to O(1) atom causes a monotonous increase in energy by ~1 kcal mol^{-1}. The PES profiles for two methods are shown in Fig. 1.

To evaluate the strength of the hydrogen bond P(2)—O(2)—H···O(1)—P(1) in compound **9**, we scanned the PES for rotation of the OH group about the O—P(2) bond. Calculations predict a monotonous increase in energy by 19.2 kcal mol^{-1} upon rotation of the hydroxyl group by 180° (Fig. 2, curve *1*). Rotation of the whole $P(2)H_2OH$ fragment about the Pt—P(2) bond (see Fig. 2, curve *2*) also leads to cleavage of the hydrogen bond; however, in this case, a local minimum cor-

Table 1. Calculated geometric parameters of type-**5** platinum complexes

Parameter	**5**	**6**		**9***	**10**	**11**
		Calculations	Experiment[10]			
Bond length			*d*/Å			
Pt(1)—P(1)	2.334	2.341	2.280	2.315 (2.343) [2.489]	2.340	2.320
Pt(1)—P(2)	2.378	2.366	2.313	2.353 (2.370) [2.344]	2.367	2.373
Pt(1)—P(3)	2.372	2.344	2.301	2.323 (2.312) [2.319]]	2.339	2.318
Pt(1)—H(1)	1.630	1.636	—	1.633 (1.619) [1.681]	1.638	1.618
O(1)—O(2)	2.462	2.455	2.317	2.470 (2.470) [2.437]	2.443	2.482
P(1)—O(1)	1.569	1.573	1.532	1.563 (1.546) [1.597]	1.574	1.546
P(2)—O(2)	1.617	1.614	1.569	1.607 (1.594) [1.571]	1.610	1.597
Bond angle			ω/deg			
P(1)—Pt(1)—P(2)	93.0	91.6	92.5	92.4	92.7	—
P(2)—Pt(1)—P(3)	107.2	102.4	100.7	98.4	101.8	—
P(1)—Pt(1)—P(3)	159.8	165.6	166.6	169.2	165.4	—
O(1)—P(1)—Pt(1)	117.2	116.8	114.9	117.3	116.5	—
O(2)—P(2)—Pt(1)	114.4	115.4	111.4	117.4	115.5	—

* The values in parentheses were obtained from B3LYP calculations; the values in brackets were obtained from MP2 calculations.

Table 2. Calculated (I) and experimental (II) geometric parameters of hydrides $[HPt(Z)(PPh_3)_2]$ with Z = CH_2CN, CF_3, Br

Parameter	CH_2CN		CF_3		Br	
	I	II[28]	I	II[29]	I	II[30]
Bond length			*d*/Å			
Pt—P	2.315	2.275	2.326	2.274	2.324	2.278
Pt—H	1.627	1.487	1.627	1.718	1.575	1.392
Pt—Z	2.197	2.16	2.135	2.009	2.590	2.535
Bond angle			ω/deg			
P—Pt—P	170.0	169.6	167.9	170.3	172.6	172.7
P—Pt—Z	95.0	95.3	95.8	94.6	93.7	93.3
P—Pt—H	86.6	—	84.1	85.0	86.3	86.5

responding to structure **12** (Fig. 3) with the energy of 13.1 kcal mol^{-1} is attained.

The high strength of the hydrogen bond in compound **9** predetermines unique properties of this chelating bidentate ligand.

Ethylene hydroformylation on complex 9. In the square-planar 16-electron complex **9**, there is an unoccupied coordination site; therefore, the addition of ethylene molecule in the first step (Eq. (7)) does not require preliminary elimination of a certain ligand and proceeds with a relative ease as the entropy-controlled reaction (ΔH_{298} = = −5.2 kcal mol^{-1}, ΔS_{298} = −41.6 e.u., ΔG_{298} = = 7.3 kcal mol^{-1}), resulting in complex **13** with the ethylene molecule coordinated to the Pt atom in η^2-fashion. Ethylene coordination is accompanied by rearrangements in the coordination site of the complex and migration of the hydrogen atom to the O(1) atom within the P(2)—O(2)—H···O(1)—P(1) chain.

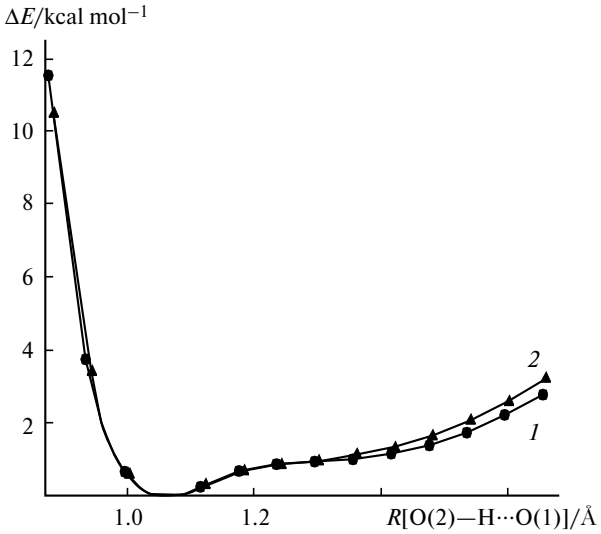

Fig. 1. Potential energy profiles obtained by scanning the O(2)—H···O(1) distance using the MP2(SDD/6-31G(d,p)) (*1*) and B3LYP(SBK/6-31G(d,p)) (*2*) methods.

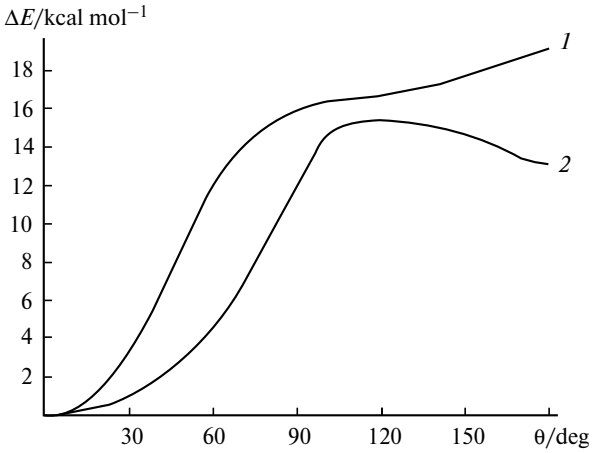

Fig. 2. Energy profile for rotation of OH group about the O—P(1) bond (*1*) and for rotation of the $P(1)H_2OH$ fragment about the Pt—P(1) bond (*2*) in complex **9**.

$$\{[(H_2PO)_2H]Pt(PH_3)(H)\} + H_2C{=}CH_2 \longrightarrow$$

9

$$\longrightarrow \{[(H_2PO)_2H]Pt(PH_3)(H)\text{-}\eta^2\text{-}(H_2C{=}CH_2)\} \quad (7)$$

13

The next step of the process, rearrangement of compound **13** to a η^1-ethyl complex **14** (Eq. (8)), proceeds *via* an early transition state TS1 with an activation energy ΔE_a° of 14.2 kcal mol^{-1}. The structures of complexes **13**, **14**, and TS1 are shown in Fig. 4.

$$\{[(H_2PO)_2H]Pt(PH_3)(H)\text{-}\eta^2\text{-}(H_2C{=}CH_2)\} \longrightarrow$$

13

$$\longrightarrow \{[(H_2PO)_2H]Pt(PH_3)CH_2CH_3\} \quad (8)$$

14

The process is exothermic (ΔH_{298} = −12.3 kcal mol^{-1}, ΔG_{298} = −13.9 kcal mol^{-1}). Ethylene insertion into the Pt—H bond is accompanied by back transfer of a hydrogen atom from the O(1) to the O(2) atom within the hydrogen bond.

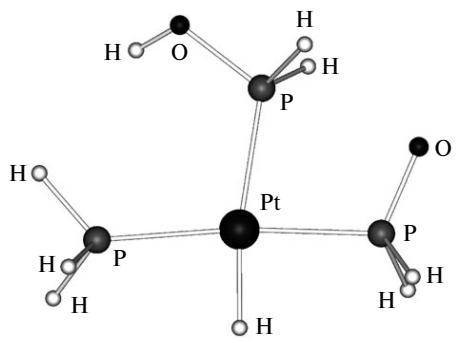

Fig. 3. Structure of complex **12**.

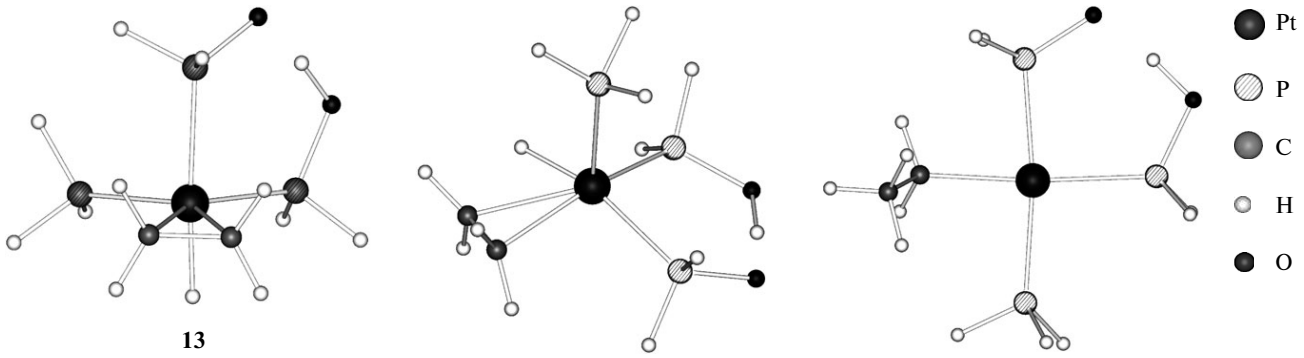

Fig. 4. Structures of complexes **13**, **14** and transition state TS1. The graphical images of atoms are valid in Figs 4—7 and 9.

The addition of carbon monoxide to compound **14** (Eq. (9)) occurs barrierlessly ($\Delta H_{298} = -10.2$ kcal mol^{-1}, $\Delta G_{298} = -0.4$ kcal mol^{-1}), resulting in complex **15** with the metal atom having a trigonal-pyramidal coordination environment (Fig. 5). Again, the process is accompanied by proton transfer within the hydrogen bond.

$$\underset{\mathbf{14}}{\{[(H_2PO)_2H]Pt(PH_3)CH_2CH_3\}} + CO \longrightarrow \underset{\mathbf{15}}{\{[(H_2PO)_2H]Pt(PH_3)(CO)CH_2CH_3\}} \quad (9)$$

This is followed by exothermic isomerization ($\Delta H_{298} = -9.0$ kcal mol^{-1}, $\Delta G_{298} = -8.9$ kcal mol^{-1}) of complex **15** to a square-planar η^1-acyl complex **16** (Eq. (10)) *via* the transition state TS2 (see Fig. 5), which requires the overcoming of the highest barrier on this reaction pathway ($\Delta E_a^\circ = 17.6$ kcal mol^{-1}). The process also involves transfer of a proton within the hydrogen bond.

$$\underset{\mathbf{15}}{\{[(H_2PO)_2H]Pt(PH_3)(CO)CH_2CH_3\}} \longrightarrow \underset{\mathbf{16}}{\{[(H_2PO)_2H]Pt(PH_3)COCH_2CH_3\}} \quad (10)$$

The oxidative addition of hydrogen molecule to compound **16** (Eq. (11)) *via* transition state TS3 results in octahedral *cis*-dihydride **17** (Fig. 6). This is an entropy-controlled process ($\Delta H_{298} = -2.0$ kcal mol^{-1}, $\Delta G_{298} = 9.7$ kcal mol^{-1}, $\Delta E_a^\circ = 12.4$ kcal mol^{-1}).

$$\underset{\mathbf{16}}{\{[(H_2PO)_2H]Pt(PH_3)COCH_2CH_3\}} + H_2 \longrightarrow \underset{\mathbf{17}}{\{[(H_2PO)_2H]Pt(H)_2(PH_3)COCH_2CH_3\}} \quad (11)$$

The catalytic cycle is closed by the exothermic ($\Delta H_{298} = -0.9$ kcal mol^{-1}, $\Delta G_{298} = -14.3$ kcal mol^{-1}) reductive elimination of propanal (Eq. (12)), which involves regeneration of the starting hydride **9**.

$$\underset{\mathbf{17}}{\{[(H_2PO)_2H]Pt(H)_2(PH_3)COCH_2CH_3\}} \longrightarrow \underset{\mathbf{9}}{\{[(H_2PO)_2H]Pt(H)(PH_3)\}} + C_2H_5COH \quad (12)$$

This step proceeds *via* transition state TS4 (Fig. 7) with an activation energy of 15.5 kcal mol^{-1}.

The complete optimum catalytic cycle of ethylene hydroformylation on type-**5** complexes is shown in Scheme 1.

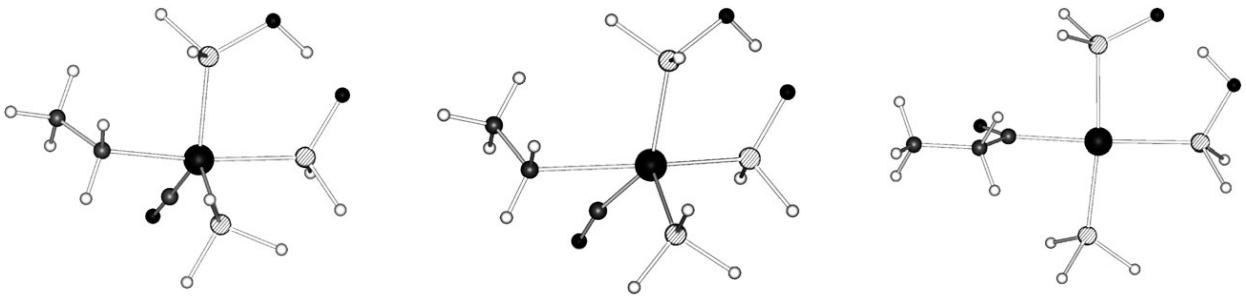

Fig. 5. Structures of complexes **15**, **16** and transition state TS2.

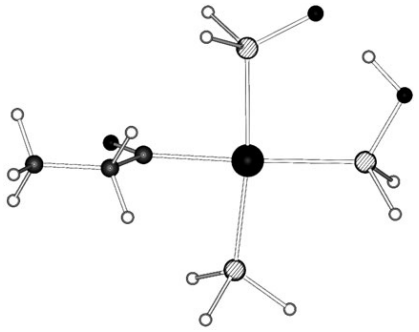

16

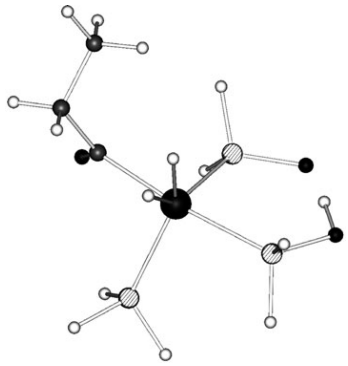

TS3

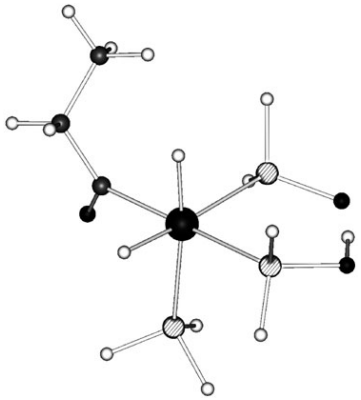

17

Fig. 6. Structures of complexes **16**, **17** and transition state TS3.

According to calculations, no steps of the catalytic cycle involve the formation of highly reactive 14-electron platinum complexes. The energy diagram of the overall process is shown in Fig. 8.

Competing hydrogenation reaction. Hydrogenation of alkenes is the main competing side process in the hydroformylation of alkenes. In particular, in the hydroformylation of hept-2-ene on complex **5** the yield of alkane can be as high as 19%, while ethylene hydrogenation on this complex proceeds at a high rate in benzene (95 °C, 20 bar).[9]

This can occur by the oxidative addition of hydrogen molecule to compound **14** followed by elimination of ethane molecule. According to calculations, the addition

Scheme1

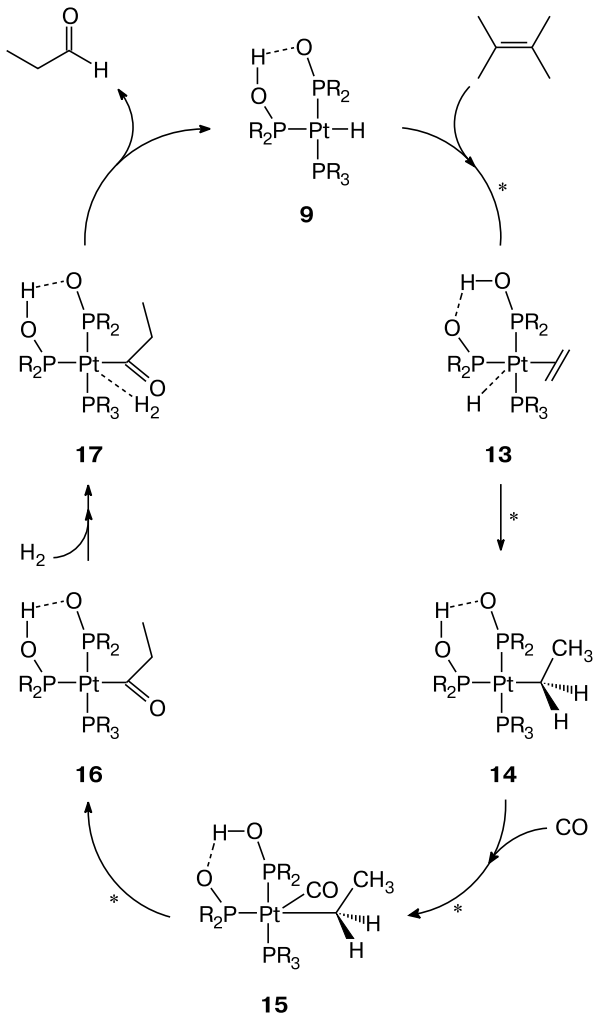

* Shown are the steps involving proton migration within the $-PR_2O-H\cdots O-PR_2$ hydrogen bond.

of H_2 to compound **14** proceeds *via* transition state TS5 with an activation energy of 14.2 kcal mol^{-1} and results in dihydride **18** (Eq. (13), Fig. 9). The process is entropy-controlled and endothermic (ΔH_{298} = 1.4 kcal mol^{-1}, ΔS_{298} = −32.6 e.u., ΔG_{298} = 11.1 kcal mol^{-1}).

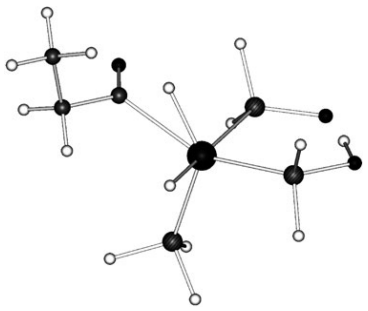

Fig. 7. Structure of transition state TS4.

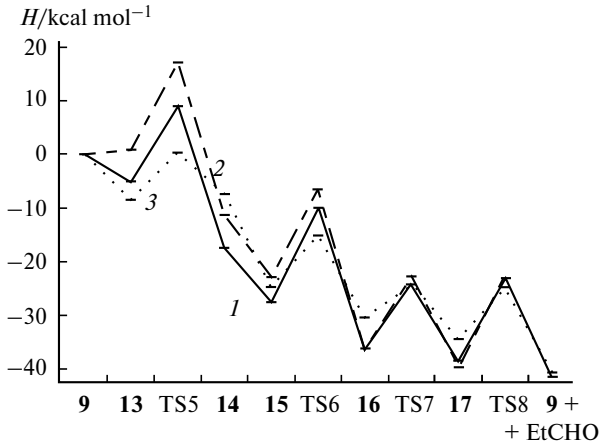

Fig. 8. Enthalpy profile along the reaction coordinate of hydroformylation on complexes **9** (*1*), **10** (*2*), and **11** (*3*); the structures and transition states are numbered as applied to complex **9**.

$$\{[(H_2PO)_2H]Pt(PH_3)CH_2CH_3\} + H_2 \longrightarrow$$

14

$$\longrightarrow \{[(H_2PO)_2H]Pt(PH_3)(H)_2CH_2CH_3\} \qquad (13)$$

18

Subsequent elimination of ethane from compound **18** (Eq. (14)) smoothly occurs *via* the transition state TS6 (see Fig. 9) with an activation energy of 13.9 kcal mol^{-1} as a strongly exothermic reaction ($\Delta H_{298} = -18.6$ kcal mol^{-1}, $\Delta G_{298} = -30.3$ kcal mol^{-1}).

$$\{[(H_2PO)_2H]Pt(PH_3)(H)_2CH_2CH_3\} \longrightarrow$$

18

$$\longrightarrow \{[(H_2PO)_2H]Pt(PH_3)H\} + C_2H_6 \qquad (14)$$

9

Although the competitive addition of CO to compound **14** (see Eq. (9)) occurs barrierlessly and is exothermic, the low barriers to the last-mentioned two reactions show that the reaction mixture should not contain excess molecular hydrogen, whereas a small excess of CO is favorable for suppression of the side process.

Effects of substituents at the phosphorus atom on the thermodynamic parameters of the process. Our study showed that ethylene hydroformylation on the model complexes **10** and **11** follows the pattern specified by complex **9**. Table 3 lists the thermodynamic parameters of the processes on all the three model complexes as well as the steps involving proton migrations within the $PR_2O—H\cdots O—PR_2$ hydrogen bonds. The energy diagrams of the processes are shown in Fig. 8. The experimentally determined enthalpy of ethylene hydroformylation calculated as the difference between the enthalpy of propanal CH_3CH_2CHO and those of the starting compounds (CO, $H_2C{=}CH_2$ and H_2) is −28 kcal mol^{-1} (see Ref. 31). The ΔG_{298} and ΔH_{298} values for this reaction calculated using standard thermodynamic data[32] are −31.3 and −14 kcal mol^{-1}, respectively. The values obtained from our calculations are significantly overestimated, which is rather typical of the density functional methods.[20] However, as was shown earlier[20] in calculations of a complete catalytic cycle of ethylene hydroformylation on the model complex $HRh(PH_3)_2CO$ using the density functional method (B3LYP) and the coupled clusters method CCSD(T), the former method quite correctly reproduces the barriers to particular steps. In this connection, the results of our calculations are suitable for qualitative assessment of the effects of substituents at the phosphorus atoms.

From the data in Table 3 (see also Fig. 8) one can see that the addition of electron-withdrawing groups to the phosphorus atoms in the complexes reduces the barriers to all steps. The first, third, fourth, and sixth steps become more exothermic, but the second step corresponding to the formation of σ-ethyl complexes becomes much more endothermic. Contrary to this, the addition of donor methyl groups causes the barriers to increase. Taking into account the fact that the electron-withdrawing substituents will undoubtedly enhance the stability of ligands and complexes against oxidation, it is clear that the design of more efficient catalytic systems for hydroformylation of alkenes based on this type of complexes requires the use of

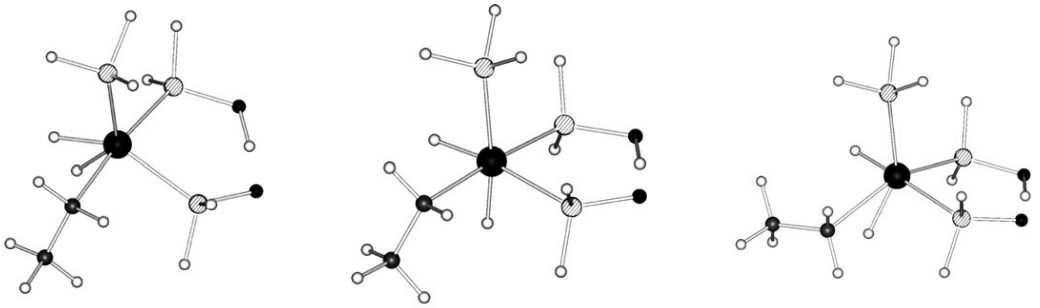

Fig. 9. Structures of complex **18** and transition states TS5 and TS6.

Table 3. Calculated ΔG_{298} (kcal mol^{-1}) and ΔH_{298} (kcal mol^{-1}) values for ethylene hydroformylation on complexes **8**, **9**, and **10**

Step	ΔG_{298}			ΔH_{298}		
	8	**9**	**10**	**8**	**9**	**10**
Ethylene addition	7.3*	12.8*	6.9	−5.2*	0.8*	−8.5
Isomerization to σ-Et-complex	−13.9*	−11.9*	2.6	−12.3*	−12.1*	1.1
CO addition	−0.4*	−1.9*	−8.5*	−10.2*	−11.6*	−17.3*
Isomerization to σ-EtCO-complex	−8.9*	−11.0*	−6.4*	−9.0*	−13.3*	−5.7*
H_2 addition	9.7	4.6*	7.3	−2.0	−3.5*	−4.0
Elimination of EtCOH	−14.3	−14.0*	−23.4	−0.9	−1.0*	−6.2
Σ	−20.5	−21.3	−21.3	−39.4	−40.6	−40.6
TS1	—	15.3	10.3	14.2	16.3	8.9
TS2	—	14.9	10.0	17.6	16.3	9.6
TS3	—	21.2	16.0	12.4	13.5	6.1
TS4	—	17.3	11.5	15.5	16.8	9.6

* Shown are the steps involving proton migration within the $—PR_2O—H\cdots O—PR_2$ hydrogen bond.

hydrophosphoryl compounds with electron-withdrawing groups at the phosphorus atoms.

Thus, our theoretical simulation of the mechanism of ethylene hydroformylation on platinum(II) complexes with hydrophosphoryl compounds allows one to determine the following factors responsible for the high efficiency and regioselectivity of the type-**5** and type-**6** complexes in the reaction in question.

1. The presence of a free coordination site in these square-planar 16-electron platinum complexes enables alkene coordination in the first step without the energetically unfavorable preliminary dissociation of a metal—ligand bond.

2. High strength of the $—PR_2O—H\cdots O—PR_2$ hydrogen bond leads to formation of a bidentate ligand in the coordination sphere of the metal. The ligand makes the geometry of the catalytic center rigid, which enhances the regioselectivity of the process.

3. The ease of migration of the highly mobile proton within the $—PR_2O—H\cdots O—PR_2$ chain provides fine adjustment of the electron density in the catalytic center in each reaction step (the proton as a molecular switch). This type of proton switches is well known in biological systems, but we failed to find information on them in metal complex systems.

Data on the effect of substituents at the phosphorus atoms in the complexes under study on the kinetic and thermodynamic parameters of the catalytic cycle are of undoubtful interest for improvement of this type of catalysts. Experiments in this field are currently in progress and their results will soon be reported elsewhere.

This work was financially supported by the Russian Foundation for Basic Research (Project No. 08-03-00586), the Federal Target Program "Research and Pedagogical Potential of Innovative Russia" (Contract 02.740.11.0266), and the Analytical Departmental Target Program "Development of Higher-School Scientific Potential" (Grant 2.1.1/4769).

References

1. E. E. Nifant´ev, *Khimiya gidrofosforil´nykh soedinenii* [*Chemistry of Hydrophosphoryl Compounds*], Nauka, Moscow, 1983, 263 pp. (in Russian).
2. D. E. C. Corbridge, *Phosphorus: An Outline of its Chemistry, Biochemistry and Uses*, Elsevier, Amsterdam, 1995, 5th ed., 336 pp.
3. J. Stawinski, A. Kraszewski, *Acc. Chem. Res.*, 2002, **35**, 952.
4. J. Chatt, B. T. Heaton, *J. Chem. Soc. A*, 1968, 2745.
5. B. Walther, *Coord. Chem. Rev.*, 1984, **60**, 67.
6. T. Appleby, J. D. Woollins, *Coord. Chem. Rev.*, 2002, **235**, 121.
7. G. Y. Li, *J. Organomet. Chem.*, 2002, **653**, 63.
8. S. P. Khanapure, D. S. Garvey, *Tetrahedron Lett.*, 2004, **45**, 5283.
9. P. W. N. M. van Leeuwen, C. F. Roobeek, R. L. Wife, J. H. G. Frijns, *J. Chem. Soc., Chem. Commun.*, 1986, 31.
10. L.-B. Han, N. Choi, M. Tanaka, *Organometallics*, 1996, **15**, 3259.
11. E. Y. Y. Chan, Q.-F. Zhang, Y.-K. Sau, S. M. F. Lo, H. H. Y. Sung, I. D. Williams, R. K. Haynes, W.-H. Leung, *Inorg. Chem.*, 2004, **43**, 4921.
12. P. Wyatt, P. Hooper, F. Sternfeld, *Tetrahedron*, 2004, **60**, 4549.
13. N. V. Dubrovina, A. Boerner, *Angew. Chem., Int. Ed.*, 2004, **43**, 5883.
14. B. Breit, W. Seiche, *J. Am. Chem. Soc.*, 2003, **125**, 6608.
15. P. W. N. M. van Leeuwen, C. F. Roobeek, US Pat. 4,408,078 Oct. 4, 1983; *Chem. Abstrs*, 1983, **99**, 121813.
16. D. G. Musaev, K. Morokuma, *Adv. Chem. Phys.*, 1996, **95**, 61.
17. W. R. Rocha, *J. Mol. Struct. (THEOCHEM)*, 2004, **677**, 133.
18. T. Ziegler, L. Cavallo, A. Berces, *Organometallics*, 1993, **12**, 3586.

19. G. Alagona, C. Ghio, R. Lazzaroni, R. Settambolo, *Organometallics*, 2001, **20**, 5394.
20. S. A. Decker, T. R. Cundari, *Organometallics*, 2001, **20**, 2827.
21. Y. V. Babin, A. V. Gavrikov, Y. A. Ustynyuk, *Mendeleev Commun.*, 2008, **18**, 12.
22. J. P. Perdew, K. Burke, M. Ernzerhof, *Phys. Rev. Lett.*, 1996, **77**, 3865.
23. D. N. Laikov, *Chem. Phys. Lett.*, 1997, **281**, 151.
24. D. N. Laikov, Yu. A. Ustynyuk, *Izv. Akad. Nauk, Ser. Khim.*, 2005, 804 [*Russ. Chem. Bull., Int. Ed.*, 2005, **54**, 820].
25. W. J. Stevens, H. Basch, M. Krauss, *J. Chem. Phys.*, 1984, **81**, 6026.
26. W. J. Stevens, M. Krauss, H. Basch, P. G. Jasien, *Can. J. Chem.*, 1992, 612.
27. T. R. Cundari, W. J. Stevens, *J. Chem. Phys.*, 1993, **98**, 5555.
28. A. Del Pra, E. Forsellini, G. Bombieri, R. A. Michelin, R. Ros, *J. Chem. Soc., Dalton Trans.*, 1979, 1862.
29. R. A. Michelin, R. Ros, G. Guadalupi, G. Bombieri, F. Benetollo, G. Chapuis, *Inorg. Chem.*, 1989, **28**, 840.
30. S. Aldridge, D. Coombs, C. Jones, *Acta Crystallogr., Sect. E: Struct. Rep. Online*, 2003, **59**, m584.
31. B. Cornils, in *New Synthesis with Carbon Monooxide*, Ed. J. Falbe, Springer Verlag, New York, 1980.
32. *Kratkii spravochnik fiziko-khimicheskikh velichin* [*A Concise Handbook of Physicochemical Data*], Eds K. P. Mishchenko and A. A. Ravdel´, Khimiya, Leningrad, 1974, 200 pp. (in Russian).

Received July 27, 2009